



## OPTIMIZATION OF TMD PARAMETERS FOR EARTHQUAKE VIBRATIONS OF TALL BUILDINGS INCLUDING SOIL STRUCTURE INTERACTION

A. Farshidianfar<sup>\*,†</sup> and S. Soheili

Mechanical Engineering Department, Ferdowsi University of Mashhad, Mashhad, Iran

### ABSTRACT

This paper investigates the optimized parameters of Tuned Mass Dampers (TMDs) for high-rise structures considering Soil Structure Interaction (SSI) effects. Three optimization methods, namely the ant colony optimization (ACO) technique together with artificial bee colony (ABC) and shuffled complex evolution (SCE) methods are utilized for the optimization of TMD Mass, damping coefficient and spring stiffness as the design variables. The objective is to decrease the maximum displacement of structure. The 40 story structure with three soil types is employed to design TMD for six types of far field earthquakes. The results are then utilized to obtain relations for the optimized TMD parameters with SSI effects. The relations are then applied to design TMD for the same structure with another five types of far field oscillations, and reasonable results are achieved. For further investigations, the obtained relations are utilized to design TMD for a new structure, and the reduction values are obtained for five types of earthquakes, which show acceptable results. This study improves the understanding of earthquake oscillations, and helps the designers to achieve the optimized TMD for high-rise buildings.

Received: 20 January 2013 Accepted: 18 July 2013

**KEY WORDS:** tuned mass damper (TMD), soil-structure interaction (SSI), ant colony optimization (ACO), artificial bee colony (ABC), shuffled complex evolution (SCE), curve fitting.

### 1. INTRODUCTION

---

\*Corresponding author: A. Farshidianfar, Professor, Mechanical Engineering Department, Ferdowsi University of Mashhad, Vakilabad Blvd., Mashhad, Iran

†E-mail address: farshid@um.ac.ir (A. Farshidianfar)

In recent years, the construction of new high-rise buildings are facilitated and developed in many countries due to the lighter and stronger materials. Since these structures are usually subjected to the earthquake vibrations, the study of tall buildings vibration mitigation and various absorbers has attracted the interest of many researchers. The tuned mass damper (TMD) is one of the simplest and the most reliable control devices among the numerous passive control methods. The main idea of employing a TMD is to produce a supplementary system that can absorb energy from the main system. The TMD technology uses a mass-spring system which oscillates with the structure, and an additional damper that connects two relatively moving points when the building oscillates. In this way, a large amount of the structural vibrating energy is transferred to the TMD and then dissipated by the damping as the primary structure is subjected to external disturbances, like earthquake and wind oscillations.

This system absorbs the vibrations automatically, and in this way the safety of the structure are greatly improved and the protected system can endure excessive vibrations and loading episodes, which can result in damage and even in failure of structural elements and equipment in the absence of TMD.

Many researchers have studied the applicability of TMDs for structures subjected to seismic excitation such as Villaverde and Koyoama [1], Rana and Soong [2], Lin et al. [3] and Wang et al. [4].

In order to develop the efficiency of control strategy, it is important to find the optimum mechanical parameters (i.e. the optimum tuning frequency, damping and mass ratio) of TMD. Several design formulas for the optimum parameters of a TMD, for different types of oscillations, have been proposed. Brock [5] and Den Hartog [6] explained the estimation of the optimum parameters of the TMD for an undamped structure subjected to harmonic external excitation. Since then, many optimum design methods of TMD have been developed to control the structural vibrations induced by various types of excitation sources, such as Crandall and Mark [7], and Rana and Soong [2]. On the basis of Den Hartog's method, Warburton and Ayorinde [8] obtained the optimized parameters of the TMD for an undamped structure under harmonic support excitation, where the acceleration amplitude is set to be constant for all input frequencies, and also for other kinds of harmonic excitations. Later, Sadek et al. [9] presented some formulations for computing the optimal parameters of TMD device based on the equal damping of the first two modes of system.

However, the optimum parameters of TMD are determined through parametric studies, or by their proposed optimum design methods. Moreover, the external disturbances considered in these studies are usually limited to white noise and harmonic forces over a frequency range. Actually, random signals such as earthquake excitations; are considered in few works, such as references [9,10].

In fact, many structures are built on soft soil where the soil-structure interaction (SSI) effect may be significant. It is well known that the SSI effects would significantly modify the dynamic characteristics of structures such as natural frequencies, damping ratios and mode shapes [11]. Xu and Kwok [12] investigated the wind-induced motion of two tall structures mounted with TMD, considering the effect of soil compliancy under the footing. They believed that soil compliancy will affect structural responses as well as the TMD effectiveness. Wu et al. [13] focused on the TMD seismic performance for structures of shallow foundations. They performed numerical investigations for a specific TMD-structure (with height of 45 m)

system built on soils with various shear wave velocities. Recently, Liu et al. [14] developed a mathematical model for time domain analysis of wind induced oscillations of a tall building with TMD considering soil effects.

However, the proposed elastic half-space model without considering material damping for soil which was not satisfied for seismic application was questionable. Moreover, the past studies on TMD used for seismic applications in structures, have not considered the effects of the altered properties of the structure due to SSI, on the performance of the damper.

Although numerous works are performed concerning SSI effects, few investigations are carried out on the time response of high-rise buildings due to earthquake excitations. In fact, the earthquake time response of tall buildings has usually been calculated employing fixed base models or single degree of freedom (SDOF) system. These analyzes cannot reasonably predict the structural responses. Moreover, the optimal parameters of TMD are extremely related to the soil type. Therefore, the time domain analysis of structures consisting SSI effects is an advantageous process for the better understanding of earthquake oscillations and TMD devices. Furthermore, few works have considered and employed heuristic algorithms, while the heuristic techniques such as Ant Colony Optimization (ACO) method, can be effectively employed for the optimized design of TMDs.

In this paper, a mathematical model is developed for calculating the earthquake response of a high-rise building with TMD. The model is employed to obtain the time response of 40 story building using TMD. The ant colony optimization (ACO) method together with artificial bee colony (ABC) and shuffled complex evolution (SCE) techniques are applied on the model to obtain the best TMD parameters. The parameters are calculated with and without soil structure interaction (SSI) effects. The effects of different parameters such as mass, damping coefficient, spring stiffness, natural frequency and damping ratio are investigated.

## 2. MODELING OF HIGH-RISE STRUCTURES

Figure 1 shows a N-story structure with a TMD and SSI effects. Mass and Moment of inertia for each floor are indicated as  $M_i$  and  $I_i$ , and those of foundation are shown as  $M_0$  and  $I_0$ , respectively. The stiffness and damping between floors are assumed as  $K_i$  and  $C_i$ , respectively.  $M_{TMD}$ ,  $K_{TMD}$  and  $C_{TMD}$  are the related parameters for TMD. Damping of the swaying and rocking dashpots are represented as  $C_s$  and  $C_r$ , and the stiffness of corresponding springs are indicated as  $K_s$  and  $K_r$ , respectively. Time histories of displacement and rotation of foundation are respectively defined as  $X_0$  and  $\theta_0$ , and displacement of each story is shown as  $X_i$ .

Using Lagrange's equation, the equation of motion for a building shown in Figure 1 can be represented as follows [15]:

$$[m]\{\ddot{x}(t)\}+[c]\{\dot{x}(t)\}+[k]\{x(t)\}=-[m^*]\{1\}\ddot{u}_g \quad (1)$$

where  $[m]$ ,  $[c]$  and  $[k]$  denote mass, damping and stiffness of the oscillating system, respectively.  $[m^*]$  indicates acceleration mass matrix for earthquake and  $\ddot{u}_g$  is the earthquake acceleration. Considering SSI effects, the N-story structure is a N+3 degree-of-freedom

oscillatory system. For such building, the mass matrix is obtained by employing Lagrange's equation in the following form [14, 15]:

$$[m] = \begin{bmatrix} [M]_{N \times N} & \{0\}_{N \times 1} & [M]_{N \times 1} & [MZ]_{N \times 1} \\ & M_{TMD} & M_{TMD} & M_{TMD}Z_N \\ & & M_0 + \sum_{j=1}^N M_j + M_{TMD} & \sum_{j=1}^N M_j Z_j + M_{TMD}Z_N \\ \text{symmetry} & & & I_0 + \sum_{j=1}^N (I_j + M_j Z_j^2) + M_{TMD}Z_N^2 \end{bmatrix} \quad (2)$$

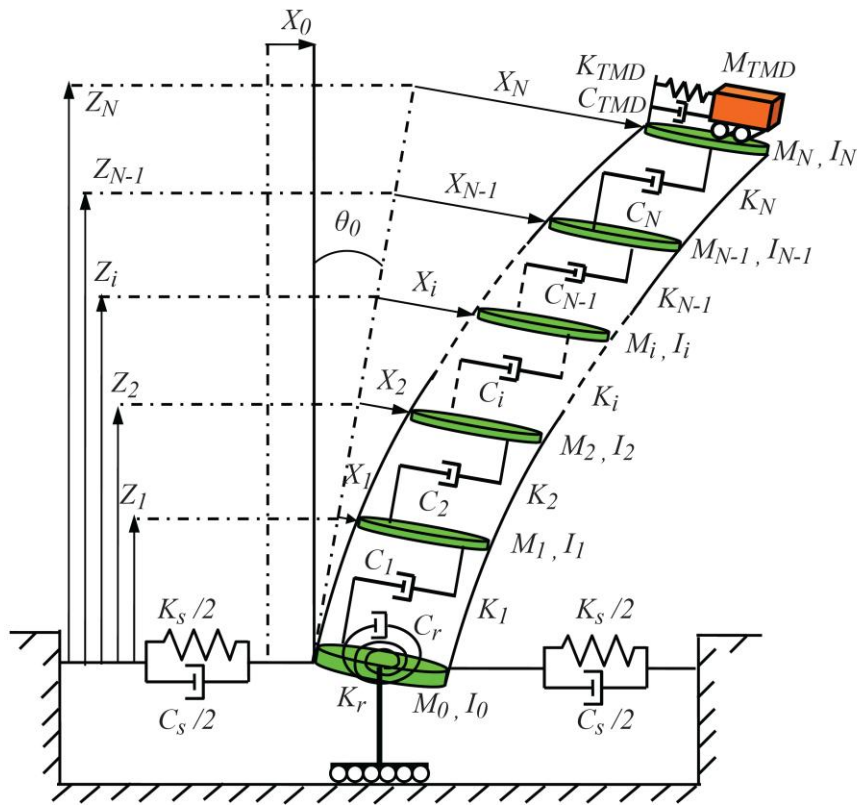


Figure 1. Shear building configuration

where

$$[M]_{N \times N} = \begin{bmatrix} M_1 & 0 & 0 & 0 & 0 \\ & M_2 & 0 & 0 & 0 \\ & & \dots & \{0\} & \{0\} \\ & & & M_{N-1} & 0 \\ \text{symmetry} & & & & M_N + M_{TMD} \end{bmatrix} \quad (3)$$

$$[M]_{N \times 1} = \begin{bmatrix} M_1 \\ M_2 \\ \vdots \\ M_{N-1} \\ M_N + M_{TMD} \end{bmatrix} \quad (4)$$

$$[MZ]_{N \times 1} = \begin{bmatrix} M_1 Z_1 \\ M_2 Z_2 \\ \vdots \\ M_{N-1} Z_{N-1} \\ (M_N + M_{TMD}) Z_N \end{bmatrix} \quad (5)$$

Using Lagrange's equation, the stiffness matrix is achieved as follows [14, 15]:

$$[k] = \begin{bmatrix} [K]_{N \times N} & \{0\}_{N \times 1} & \{0\}_{N \times 1} & \{0\}_{N \times 1} \\ & K_{TMD} & 0 & 0 \\ & & K_s & 0 \\ \text{symmetry} & & & K_r \end{bmatrix} \quad (6)$$

In which:

$$[K]_{N \times N} = \begin{bmatrix} K_1 + K_2 & -K_2 & 0 & 0 & 0 \\ & K_2 + K_3 & 0 & 0 & 0 \\ & & \dots & \vdots & \{0\} \\ & & & K_{N-1} + K_N & -K_N \\ \text{symmetry} & & & & K_N \end{bmatrix} \quad (7)$$

Similarly, the damping matrix can be stated in the following form:

$$[c] = \begin{bmatrix} [C]_{N \times N} & \{0\}_{N \times 1} & \{0\}_{N \times 1} & \{0\}_{N \times 1} \\ & C_{TMD} & 0 & 0 \\ & & C_s & 0 \\ \text{symmetry} & & & C_r \end{bmatrix} \quad (8)$$

where:

$$[C]_{N \times N} = \begin{bmatrix} C_1 + K_2 & -C_2 & 0 & 0 & 0 \\ & C_2 + C_3 & 0 & 0 & 0 \\ & & \dots & \vdots & \{0\} \\ & & & C_{N-1} + C_N & -C_N \\ \text{symmetry} & & & & C_N \end{bmatrix} \quad (9)$$

Finally, the acceleration mass is obtained as follows:

$$[m^*] = \begin{bmatrix} [M]_{N \times N} & \{0\}_{N \times 1} & \{0\}_{N \times 1} & \{0\}_{N \times 1} \\ 0 & M_{TMD} & 0 & 0 \\ 0 & 0 & M_0 + \sum_{j=1}^N M_j + M_{TMD} & 0 \\ 0 & 0 & \sum_{j=1}^N M_j Z_j + M_{TMD} Z_N & 0 \end{bmatrix} \quad (10)$$

Ignoring the SSI effects, rows and columns  $N+2$  and  $N+3$  are neglected, and the mentioned matrices are reduced to  $(N+1) \times (N+1)$  dimensional matrices.

According to Rayleigh proportional damping, the damping matrix of  $N$ -story structure can be represented as follows:

$$[c]_{N \times N} = A_0 [m]_{N \times N} + A_1 [k]_{N \times N} \quad (11)$$

in which  $A_0$  and  $A_1$  are Rayleigh damping coefficients.

The displacement vector  $\{x(t)\}$  including both displacement and rotation of floors and foundation as well as TMD motion can be represented as follows:

$$\{x(t)\} = \{X_1(t) \ X_2(t) \ \dots \ X_N(t) \ X_{TMD}(t) \ X_0(t) \ \theta_0(t)\}^T \quad (12)$$

The parameters  $C_s$ ,  $C_r$ ,  $K_s$  and  $K_r$  can be obtained from soil properties (i.e. poisson's ratio  $\nu_s$ , density  $\rho_s$ , shear wave velocity  $V_s$  and shear modulus  $G_s$ ) and radius of foundation  $R_0$  [14]. In this paper, Tabas and Kobe earthquakes acceleration spectra are applied to the structure, and time response of TMD and building are calculated based on Newmark integration method [16].

### 3. ANT COLONY OPTIMIZATION (ACO) METHOD

In order to obtain the best parameters for TMD, the ant colony optimization (ACO) is employed. This algorithm firstly proposed by Dorigo and Gambardella [17] is based on the behavior of ants finding the shortest paths from a food source to their nest only by sensing the intensity of pheromone deposited by other ants. It is observed that they usually select the path with higher pheromone. This mechanism makes the shorter paths more desirable as it takes shorter time to march on them.

This behavior is simulated by three rules in ACO algorithm, which was originally applied on combinatorial problems with discrete variables such as Traveling Salesman or Quadratic Assignment. Recently, this method is employed by Kaveh and Talataheri [18, 19] to optimize truss structures with discrete variables. For engineering problems and where the design variables are usually continuous, the method of discretization is an acceptable approach [20]. Once the continuous variables are divided into separated domains, the problem can be treated as a problem with discrete variables.

Regarding the discretization procedure, the design variables are presented by  $i$  and their divided search domains are shown by  $j$ . The sections of total solution are chosen in a constructive approach named as “state transition rule”:

$$S = \begin{cases} \arg \max \{ [\tau(i, j)] \cdot [\eta(i, j)]^\beta \} & \text{if } q \leq q_0 \\ s & \text{otherwise} \end{cases} \quad (13)$$

where  $\tau(i, j)$  shows the amount of pheromone related to the  $j$ th element of variable  $i$ , and  $\eta(i, j)$  is the heuristic function defined according to the investigated problem. In this rule,  $q$  is a random number, and  $q_0$  is a parameter set by the user ( $0 \leq q, q_0 \leq 1$ ). If  $q > q_0$ , the next step is selected according to proportional distribution of probability function, like the roulette wheels, assigned as follows:

$$s = \begin{cases} \frac{[\tau(i, j)] \cdot [\eta(i, j)]^\beta}{\sum_{u \in \text{allowed } u} [\tau(i, u)] \cdot [\eta(i, u)]^\beta} & \text{if } j \in \text{allowed } j \\ 0 & \text{otherwise} \end{cases} \quad (14)$$

The significant factor of  $q_0$  defines the range of randomness against determination of state transition rule. It is clear that the higher amount of  $q_0$  directs the algorithm towards deterministic decisions, while the lower amounts generates more randomness.

To avoid stagnation of the algorithm and similar to evaporation of pheromone in real world, the amount of pheromone level is changed after finishing each evaluation by applying “the local updating rule”:

$$\tau(i, j) = (1 - \rho) \cdot \tau(i, j) + \rho \cdot \Delta \tau(i, j) \quad (15)$$

where  $\rho$  denotes the local evaporation coefficient. The best performance is obtained when  $\Delta \tau(i, j) = \tau_0$  [17].

The third rule known as “the global updating rule” acts as a positive feedback and accumulates more pheromone around the best solution obtained so far:

$$\tau(i, j) = (1 - \alpha) \cdot \tau(i, j) + \alpha \cdot \Delta \tau \quad (16)$$

where  $\Delta\tau$  is the inverse of the objective function and  $\alpha$  is the global evaporation coefficient [17].

This process of evaluation and updating is repeated with  $n$  ants until the termination condition, which is usually the maximum number of cycles, is satisfied. Similar to other heuristic optimization techniques, it is important to tune the algorithm to achieve sensible results. For the tackled problem in this paper, the values presented in Table 1 are found acceptable. In addition, without damaging the overall effectiveness of ACO [17], the heuristic function is neglected due to intricacies in its definition procedure.

In this paper, the objective is to minimize the maximum displacement of the whole structure.

#### 4. ARTIFICIAL BEE COLONY (ABC) METHOD

Natural behavior of bees and their collective activities in their hives has been fascinating researchers for centuries. Artificial Bee Colony (ABC) algorithm, the method employed in this paper, was presented by Karaboga [21] to optimize numeric benchmark functions. It was then extended by Karaboga and Basturk and showed to outperform other recognized heuristic methods such as GA [22].

In this model, the honey bees are categorized as employed, onlooker and scout. An employed bee is a forager associated with a certain food source which she is currently exploiting. An onlooker bee is an unemployed bee at the hive which tries to find a new food source using the information provided by employed bees. A scout, ignoring the other's information, searches around the hive randomly.

In ABC, the solution candidates are modeled as food sources and their corresponding objective functions as the quality (nectar amount) of the food source. For the first step, the artificial employed bees are randomly scattered in the search domain producing  $SN$  initial solutions. After this initialization, the main loop of the algorithm described hereafter is repeated for a predetermined number of cycles or until a termination criterion is satisfied.

Firstly, all employed bees attempt to find new solutions in the neighbor of the solution (food source) they memorized at the previous cycle. If the quality (the amount of objective function) is higher at this new solution, then she forgets the former and memorizes the new one. In ABC, a particular mechanism is devised for this purpose:

$$v_{ij} = x_{ij} + \phi_{ij}(x_{ij} - x_{kj}) \quad (17)$$

where  $j \in \{1, 2, \dots, D\}$  and  $k \in \{1, 2, \dots, SN\}$  are randomly chosen indices, and  $v_{ij}$  represents the new solution (new food source position). It should be noted that  $k \neq i$ . The parameter  $\phi_{ij}$  is also a random number in the domain  $[-1, 1]$ .

After that, the onlooker bees should select the solution around which they explore for new food sources. This is performed probabilistically i.e. a mechanism like roulette wheel is employed. With the help of a uniform random number generator, the solutions for further exploration can be easily determined:



$$p_i = \frac{fit_i}{\sum_{n=1}^{SN} fit_n} \quad (18)$$

Additionally, updating food sources is done with the same greedy process by comparing the new solutions produced by onlookers and the corresponding current solutions. It is notable that different approaches have been proposed for assigning fitness to solutions. Basturk and Karaboga[23] has utilized a familiar form described below which is adopted in this paper as well:

$$fit_i = \begin{cases} \frac{1}{1+f_i} & f_i \geq 0 \\ 1+|f_i| & f_i < 0 \end{cases} \quad (19)$$

where  $f_i$  is the objective function of solution  $x_i$ .

If a solution can not be improved by employed or onlooker bees after certain iterations called *limit*, then the solution is abandoned and the bee becomes a scout, which searches randomly for a new solution within the search space. It should be reminded that at each cycle, only one artificial bee is allowed to become scout and perform the search as follows:

$$x_i^j = x_{\min}^j + \varphi(x_{\max}^j - x_{\min}^j) \quad (20)$$

where  $\varphi$  is a random number in domain [0, 1]. Obviously, variables of all dimensions are replaced with new randomly-generated values.

## 5. SHUFFLED COMPLEX EVOLUTION (SCE) METHOD

The shuffled complex evolution (SCE) method is another effective and robust algorithm finds a global minimum of a function with several variables. It was introduced and developed by Duan et al. [24, 25] and Sorooshian et al. [26].

A general description of the steps of the SCE method is explained as follows.

(1) Sample generation -- random sampling of  $s$  points in the feasible parameter domain and calculating the objective function for each point. If there is no prior information on the approximate position of the global optimum, a uniform probability distribution is used to generate a sample.

(2) Point ranking -- sorting the  $s$  points in order of rising objective value in such a way that the first point shows the least objective value and the last one signifies the greatest objective value.

(3) Complex partitioning -- partitioning the  $s$  points into  $p$  complexes, each contains  $m$  points. The complexes are divided such that the first complex includes  $p(k - 1) + 1$  ranked points, the second complex includes  $p(k - 1) + 2$  ranked points, and so on, where  $k = 1, 2,$

...,  $m$ .

(4) Complex development -- developing each complex according to the competitive complex evolution (CCE) algorithm. This algorithm operates based on the Nelder and Mead [27] Simplex downhill search scheme.

(5) Complex shuffling -- combining the points in the developed complexes into a single sample population; sorting the sample population in order of rising objective value; and shuffling (i.e. re-partitioning) the sample population into  $p$  complexes considering the procedure described in Step (3).

(6) Convergence checking -- stop if any of the defined convergence criteria is satisfied; continue otherwise.

(7) Checking the reduction in the number of complexes--if the minimum number of complexes essential for the population,  $P_{\min}$ , is smaller than  $p$ , remove the complex with the lowest ranked points; set  $p = p - 1$  and  $s = pm$ ; return to Step 4. If  $P_{\min} = p$  then return to Step 4.

The primary random sampling of parameter domain provides the potential for finding the global optimum without being biased by pre-specified starting points. The partitioning of the population into communities assists a freer and broader exploration of the feasible space in various directions. The shuffling of communities improves the survivability by sharing of the information (about the search space) achieved separately by each community.

## 6. ILLUSTRATIVE EXAMPLE

The methodology outlined previously is employed to calculate the structural response of a 40-story building with TMD. Table 1 shows the structure parameters [14]. The stiffness  $K_i$  linearly decreases as  $Z_i$  increases. TMD is installed on the top of building for the better damping of vibrations.

Table 1: Structure parameters [14]

No. of stories	40
Story height ( $Z_i$ )	4 m
Story mass ( $M_i$ )	$9.8 \times 10^5$ kg
Story moment of inertia ( $I_i$ )	$1.31 \times 10^8$ kgm <sup>2</sup>
Story stiffness ( $K_i$ )	$K_1 = 2.13 \times 10^9$ N/m $K_{40} = 9.98 \times 10^8$ N/m $K_{40} \leq K_i \leq K_1$
Foundation radius ( $R_0$ )	20 m
Foundation mass ( $M_0$ )	$1.96 \times 10^6$ kg
Foundation moment of inertia ( $I_0$ )	$1.96 \times 10^8$ kgm <sup>2</sup>

In this study, three types of ground states, namely soft, medium and dense soil are examined. A structure with a fixed base is also investigated. The soil and foundation properties are presented in Table 2.

Table 3 represents the first 3 natural and damped frequencies of the structure,

considering and ignoring SSI effects.

Table 2: Parameters of the soil and foundation [14]

Soil Type	Swaying	Rocking	Swaying	Rocking
	damping $C_s$ (Ns/m)	damping $C_r$ (Nsm)	stiffness $K_s$ (N/m)	stiffness $K_r$ (N/m)
Soft Soil	$2.19 \times 10^8$	$2.26 \times 10^{10}$	$1.91 \times 10^9$	$7.53 \times 10^{11}$
Medium Soil	$6.90 \times 10^8$	$7.02 \times 10^{10}$	$1.80 \times 10^{10}$	$7.02 \times 10^{12}$
Dense Soil	$1.32 \times 10^9$	$1.15 \times 10^{11}$	$5.75 \times 10^{10}$	$1.91 \times 10^{13}$

Table 3: Natural and damped frequencies of the structure

Soil Type	$\omega$	$\omega_1$ (rad/s)	$\omega_2$ (rad/s)	$\omega_3$ (rad/s)
1 Soft Soil	With Damping	-0.02i±1.08	-0.24i±4.45	-0.62i±7.42
	Without Damping	1.09	4.44	7.40
2 Medium Soil	With Damping	-0.02i±1.54	-0.21i±4.57	-0.58i±7.55
	Without Damping	1.54	4.58	7.58
3 Dense Soil	With Damping	-0.02i±1.60	-0.21i±4.58	-0.58i±7.57
	Without Damping	1.61	4.59	7.59
4 Fixed Base	With Damping	-0.03i±1.64	-0.21i±4.59	-0.58i±7.58
	Without Damping	1.65	4.60	7.60

The TMD design variables are set in such a way that all the first 3 frequencies of the structure are covered, and damping ratio ( $\zeta$ ) is always less than unity. In this way, the maximum mass ratio is about 3.5% of the first modal mass, i.e.  $50 \times 10^3 \leq M_{TMD} \leq 1000 \times 10^3$  (kg), the TMD spring stiffness is set as  $0.3 \times 10^6 \leq K_{TMD} \leq 60 \times 10^6$  (N/m) and the TMD damping is tuned to  $0.1 \times 10^3 \leq C_{TMD} \leq 2000 \times 10^3$  (Ns/m). In this way, the mass ratio is about 3.5% of the first modal mass.

As mentioned before, six types of far field earthquakes, namely Cape Mendocino, Coalinga, Imperial Valley (two earthquakes), Landers, and Loma Prieta earthquake data are employed to obtain the optimized mass ratio ( $\mu$ ), frequency ratio ( $f$ ) and damping ratio ( $\zeta$ ) for TMD device, which are defined as follows:

$$\mu = \frac{M_{TMD}}{M_s} \quad (21)$$

$$f = \frac{\omega_{TMD}}{\omega_s} \quad (22)$$

$$\zeta = \frac{C_{TMD}}{2M_{TMD}\omega_{TMD}} \quad (23)$$

where  $M_s$  relates to the first modal mass of structure based on the unit modal participation factor, and  $\omega_s$  shows the first frequency of fix based structure.

The 3 outlined optimization methods are applied to the problem to find the best values for mass, spring stiffness and damping quantity of TMD device. The results are presented in Table 4 for 6 types of earthquakes. According to this table, the ACO results evidently outperform the SCE and ABC results, while the ABC and ACO results are close together in most cases.

Table 4: Reduction percentages for 6 earthquakes using 3 optimization methods

earthquake	Soil type	$u_{\max}$ (without TMD)	%Reduction		
			ACO	ABC	SCE
Cape Mendocino	soft soil	0.3079	9.3862	9.3862	8.5008
	medium soil	0.4299	28.8439	28.0996	25.2617
	dense soil	0.3675	6.6395	9.9048	10.8571
	fixed base	0.3829	14.9647	13.9984	12.7448
Coalinga	soft soil	0.1489	42.1088	41.8402	38.0792
	medium soil	0.1637	33.4148	33.0483	29.7404
	dense soil	0.1624	34.6675	34.6675	32.2118
	fixed base	0.1684	36.5202	36.5202	35.7482
Imperial Valley (I)	soft soil	1.6350	27.8777	21.657	19.847
	medium soil	1.6291	38.1253	24.400	24.271
	dense soil	1.8179	42.2300	44.353	42.032
	fixed base	1.6372	34.5651	31.132	31.230
Imperial Valley (II)	soft soil	0.3582	46.1753	45.9799	42.3534
	medium soil	0.1980	33.8889	24.4444	21.4141
	dense soil	0.1717	29.5865	24.1701	23.4129
	fixed base	0.1690	28.1657	27.2189	25.6213
Landers	soft soil	1.3423	2.5404	11.0855	13.4396
	medium soil	0.6106	14.1828	14.1009	11.2349
	dense soil	0.5363	8.2976	8.2230	7.8273
	fixed base	0.4875	8.8205	2.4000	5.4359
Loma Prieta	soft soil	0.2464	16.9237	16.8831	16.7922
	medium soil	0.3988	58.5005	58.4002	56.0171
	dense soil	0.3080	49.2532	36.5584	35.9416
	fixed base	0.2506	40.5427	32.1229	30.1676

The convergence time history of the 3 algorithms, such as the one presented in Figure 2; reveals that the ACO method converges more rapidly and efficiently than the two other methods. This figure is plotted for 1000 evaluations of the problem. The optimization programs are performed on 2.8 GHz Core2Duo system with 4GB RAM, and the elapsed times are presented in Figure 3. According to this figure, the consumed time for ACO and ABC methods are far less than the SCE method. However, the elapsed time for ACO is slightly less than the ABC algorithm.

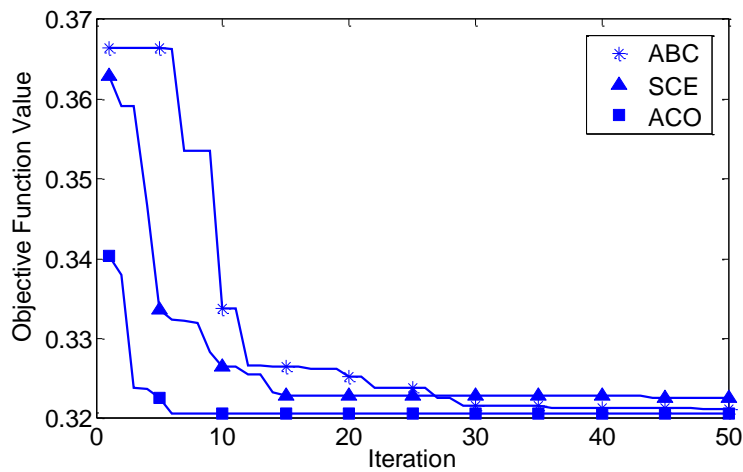


Figure 2. Convergence time history of the 3 optimization methods for Cape Mendocino earthquake considering dense soil

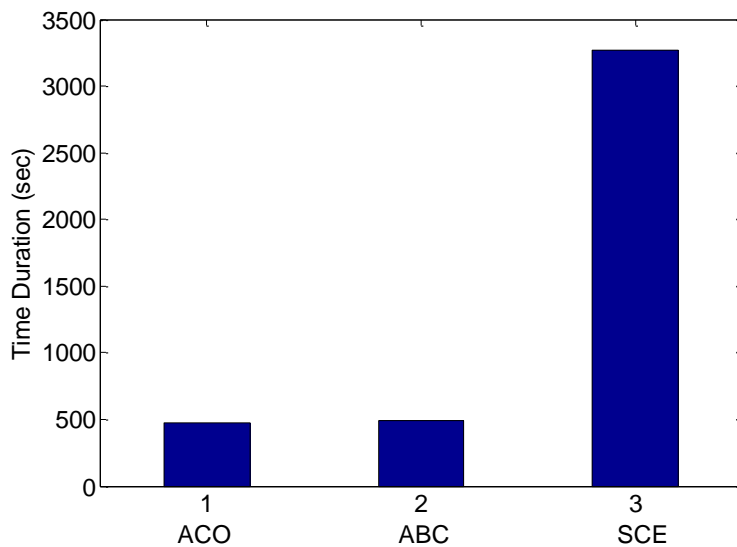


Figure 3. Consumed time for the 3 optimization methods

In accordance with the mentioned facts, it could be concluded that the ACO method is more efficient and reliable than the two other methods, therefore; it is selected as the best and basic method for the following parts of the research.

## 7. CURVE FITTING

Using the ACO method, two sets of optimized parameters ( $\mu$ ,  $f$  and  $\zeta$ ) for each soil type and earthquake are obtained. For the curve fitting, the following relation is considered for the mass ratio:

$$\mu = a_1 \mu_1^{n_1} + a_2 \mu_2^{n_2} \quad (24)$$

where:

$$\mu_1 = \frac{M_{TMD}(\text{fix based structure})}{M_s(\text{fix based structure})} \quad (25)$$

$$\mu_2 = \frac{M_s(\text{fix based structure})}{M_s(\text{structure with SSI})} \quad (26)$$

$$M_s = \Phi^T [M] \Phi \quad (27)$$

in which,  $\Phi$  represents the normalized fundamental mode shape of the structure. The coefficients  $a_1$ ,  $n_1$ ,  $a_2$  and  $n_2$  are achieved by using the ACO technique to minimize the RMS (Root Mean Square) of errors. The optimized values are obtained as follows:  $a_1 = 3.2287$ ,  $n_1 = 1.5103$ ,  $a_2 = 3.4108$ ,  $n_2 = 0.5768$ .

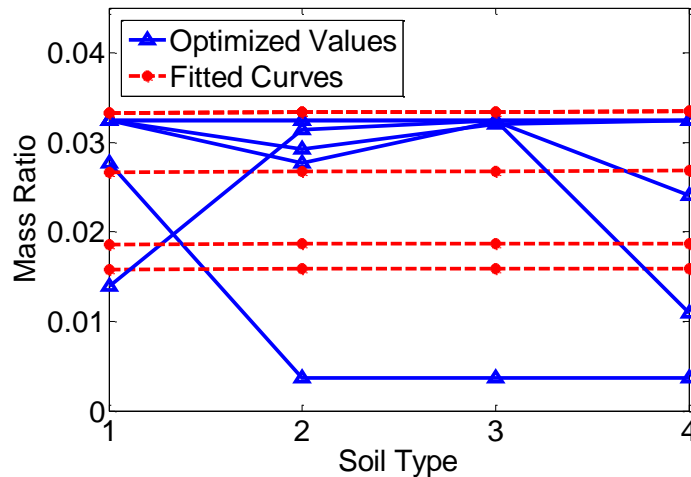


Figure 4. Optimized and fitted values for mass ratio

Figure 4 represents the optimized and fitted values for the mass ratio. According to this figure, the structure constructed on the soil with greater stiffness and damping needs TMD with smaller  $M_{TMD}$ . Considering Table 3, the soil with higher stiffness and damping brings higher natural and damped frequency, therefore; it can be concluded that the structure with higher frequency (constructed on the dense soil) requires TMD with lower mass ratio.

The similar method is employed for obtaining the proper coefficients of frequency ratio including SSI effects, which is defined in the following form:

$$f = b_1 f_1^{m_1} + b_2 f_2^{m_2} \quad (28)$$

where:

$$f_1 = \frac{1}{1 + \mu\phi} \left[ 1 - \beta \sqrt{\frac{\mu\phi}{1 + \mu\phi}} \right] \quad (29)$$

$$f_2 = \frac{C_s C_r}{K_s K_r} \quad (30)$$

The parameters  $f_1$  and  $\phi$  shows the frequency ratio and the first modal participation factor for the fix based structure, respectively; and  $\beta$  represents the damping of the structure [9]. Using the ACO method to minimize the RMS of errors, the coefficients  $b_1$ ,  $m_1$ ,  $b_2$  and  $m_2$  are obtained as follows:  $b_1 = 1.3857$ ,  $m_1 = 0.5471$ ,  $b_2 = 1.8053$ ,  $m_2 = 0.5520$

The optimized and fitted values for the frequency ratio are presented in Figure 5. The results show that the structure constructed on the soil with greater stiffness and damping requires TMD with smaller stiffness and natural frequency. According to Table 3, it can be seen that the structure with higher frequency (constructed on the dense soil) requires TMD with lower natural frequency.

In order to reach the appropriate coefficients of damping ratio considering soil effects, the similar method is applied on the best values of damping ratio obtained by ACO method. The proposed relation for damping ratio is defined in the following form:

$$\xi = c_1 \xi_1^{p_1} + c_2 \xi_2^{p_2} \quad (31)$$

in which:

$$\xi_1 = \phi \left[ \frac{\beta}{1 + \mu} + \sqrt{\frac{\mu}{1 + \mu}} \right] \quad (32)$$

$$\xi_2 = \frac{C_s C_r}{K_s K_r} \quad (33)$$

The parameter  $\xi_1$  shows the damping ratio for the fix based structure [9]. The coefficients  $c_1$ ,  $p_1$ ,  $c_2$  and  $p_2$  are obtained using the ACO method to minimize the RMS of errors. The optimized values are achieved in the following form:  $c_1 = 0.5644$ ,  $p_1 = 0.8578$ ,  $c_2 = 3.2054$ ,  $p_2 = 1.4543$

Figure 6 shows the optimized and fitted values of damping ratio. The results show that there is a close relationship between soil and optimized parameters of TMD.

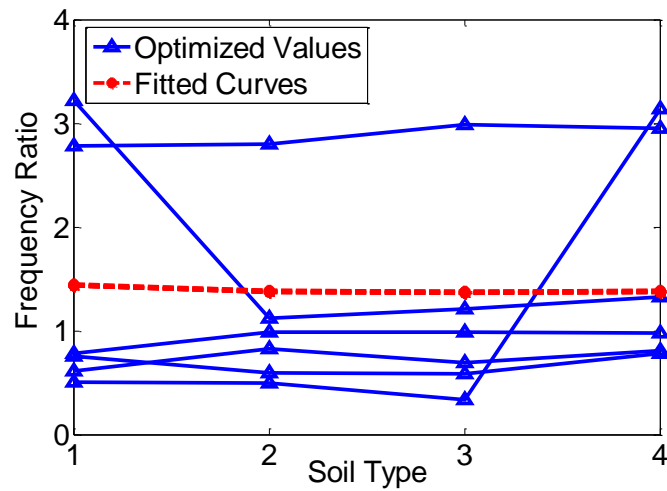


Figure 5. Optimized and fitted values for the frequency ratio

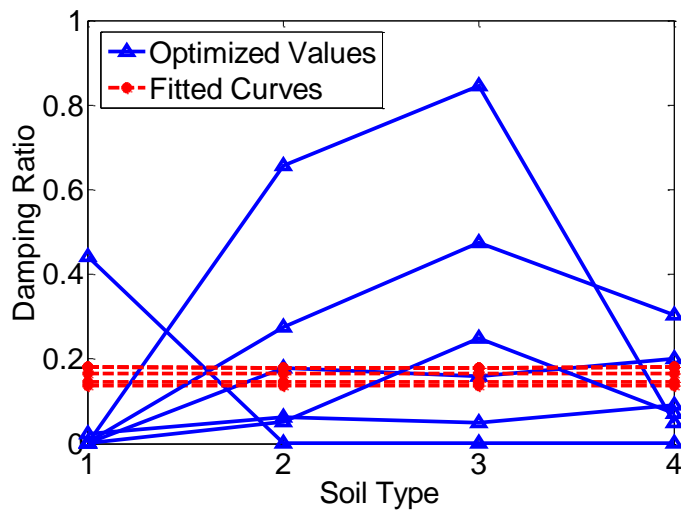


Figure 6. Optimized and fitted values for damping ratio

## 8. RESULTS AND DISCUSSIONS

The methodology outlined previously and the obtained relations are employed to design TMD for the same structure with five different types of far field earthquakes, namely Superstition Hills, San Fernando, Northridge, Chi-Chi and El-Centro seismic oscillations. By estimation of  $\mu_1=3\%$ , the real values of  $\mu$ ,  $f$ ,  $\zeta$  and therefore  $M_{TMD}$ ,  $K_{TMD}$  and  $C_{TMD}$  are calculated for each soil type. The designed TMD is then employed to decrease the displacement and acceleration of the structure.

Figure 7 shows the displacement reduction percentages for the mentioned earthquakes. It can be seen that the proposed relations result in effective reductions for all earthquakes and



different soil types. According to this figure, the TMD is more efficient for dense soil types, therefore; ignoring the soil effects (assuming the structure as fix based model) would result in overestimated outcomes.

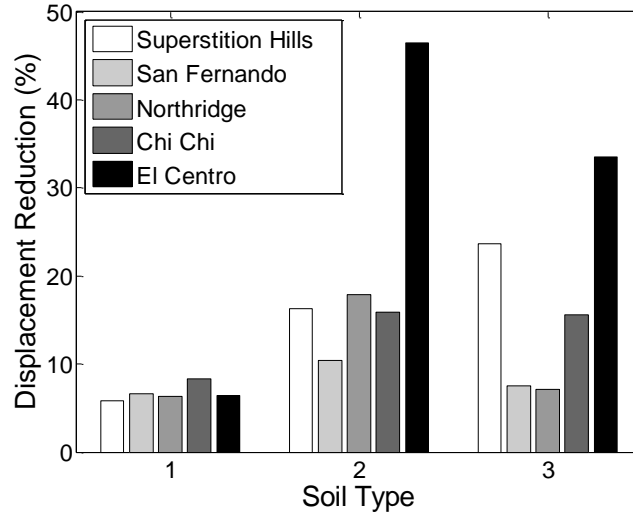


Figure 7. The displacement reduction percentage for 40 story structure

Figure 8 illustrates that the designed TMD reasonably reduced the maximum acceleration of the structure. As it can be seen from these figures, the proposed relations are result in acceptable reductions in most cases. However, there are some exceptions because the main purpose of TMD design is the reduction of displacement solely.

For further investigations, another 15 story structure is modeled and employed to design TMD for and calculate the structural response. The structure parameters are presented in Table 5 [28].

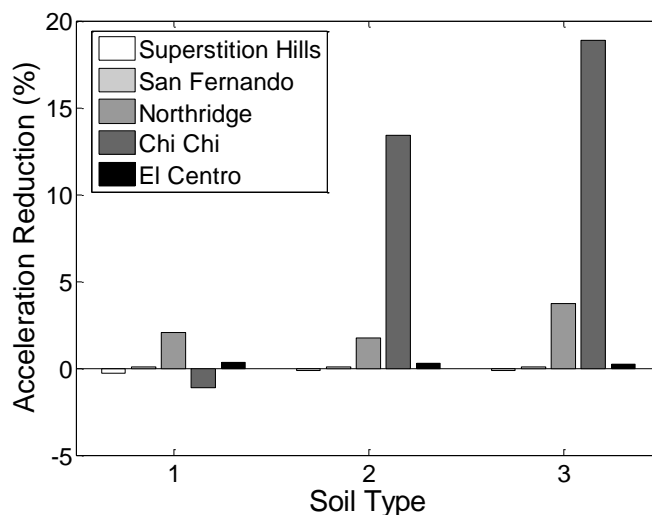


Figure 8. The acceleration reduction percentage for 40 story structure

Table 5: Structure parameters [28]

No. of stories	15
Story height ( $Z_i$ )	3.5 m
Story mass ( $M_i$ )	$M_i = 3.456 \times 10^5$ kg
	$M_1 = 4.500 \times 10^5$ kg
Story moment of inertia ( $I_i$ )	$0.146 \times 10^8$ kgm <sup>2</sup>
Story stiffness ( $K_i$ )	$K_i = 3.40 \times 10^8$ N/m
	$K_1 = 18.05 \times 10^6$ N/m
Foundation radius ( $R_0$ )	11.5 m
Foundation mass ( $M_0$ )	$0.655 \times 10^6$ kg
Foundation moment of inertia ( $I_0$ )	$0.220 \times 10^8$ kgm <sup>2</sup>

In this study, three types of ground states, namely soft, medium and dense soil are examined, using the new soil parameters. Table 6 represents the first 3 natural and damped frequencies of the structure, considering and ignoring SSI effects.

The previous methodology and the obtained relations are employed to design TMD for the new structure with 3 types of earthquakes. Estimating that  $\mu_1=3\%$ , the real values of  $\mu, f, \zeta$  and then  $M_{TMD}, K_{TMD}$  and  $C_{TMD}$  are calculated for each soil type.

The displacement reduction percentage for the mentioned earthquakes is presented in Figure 9. This figure reveals that the designed TMD by proposed relations can effectively reduce the maximum displacement of the structure.

Table 6: Natural and damped frequencies of the structure

Soil Type	$\omega$	$\omega_1$ (rad/s)	$\omega_2$ (rad/s)	$\omega_3$ (rad/s)
1 Soft Soil	With Damping	-0.004i±1.58	-0.08i±6.15	-0.08i±13.05
	Without Damping	1.58	6.15	13.05
2 Medium Soil	With Damping	-0.002i±1.64	-0.03i±6.82	-0.08i±13.05
	Without Damping	1.64	6.83	13.05
3 Dense Soil	With Damping	-0.002i±1.65	-0.02i±6.89	-0.08i±13.05
	Without Damping	1.65	6.89	13.05
4 Fixed Base	With Damping	-0.002i±1.66	-0.02i±6.92	-0.08i ±13.05
	Without Damping	1.66	6.93	13.06

Further studies reveal that the maximum acceleration is reasonably decreased except in few cases, which is because the main purpose of TMD design is to reduce the displacement solely. However, the proposed relations are result in acceptable reductions in most cases. Further structure samples and earthquakes are to be investigated for the better estimation of TMD parameters.

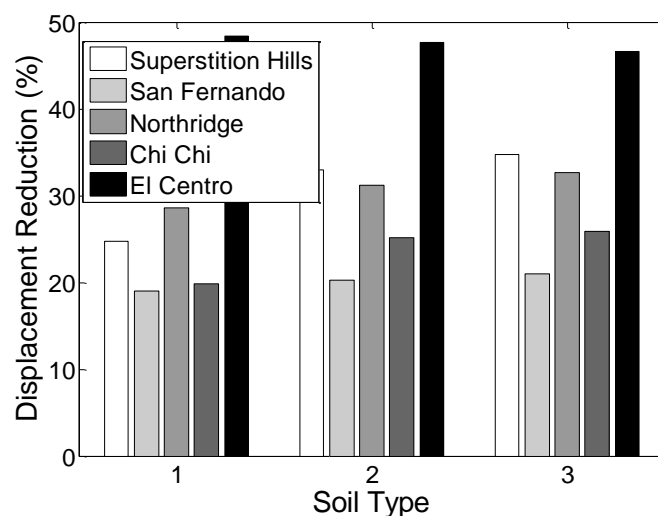


Figure 9. The displacement reduction percentage for 16 story structure

## 9. CONCLUSIONS

In this paper, the ACO, ABC and SCE techniques are utilized to modify the former relations for the optimized TMD parameters considering soil effects. The 40 story structure with three soil types is employed to design TMD in order to decrease the maximum displacement of the building for six types of far field earthquakes. Using the time domain analysis based on Newmark method; the displacement, velocity and acceleration of different stories and TMD are obtained. The optimized mass, frequency and damping ratio are then formulated for different soil types; and employed for the design of TMD parameters for the 40 and 15 story buildings and five different earthquakes, and well results are achieved. This study leads the researchers to the better understanding and designing of TMDs for the mitigation of earthquake oscillations.

## ACKNOWLEDGEMENT

This work was supported by Research Grant No. 2/18192 from Ferdowsi University of Mashhad, Mashhad, Iran.

## REFERENCES

1. Villaverde R, Koyoama LA. Damped resonant appendages to increase inherent damping in buildings, *Earthquake Eng Struct Dynam*, 1993; **22**: 491–507.
2. Rana R, Soong TT. Parametric study and simplified design of tuned mass dampers, *J*

- Struct Eng*, 1998; **20**(3): 193–204.
3. Lin CC, Ueng JM, Huang TC. Seismic response reduction of irregular buildings using passive tuned mass dampers, *Eng Struct*, 2000; **22**(5): 513–524.
  4. Wang AP, Fung RF, Huang SC. Dynamic analysis of a tall building with a tuned-mass-damper-device subjected to earthquake excitations, *J Sound Vib*, 2001; **244**(1): 123–136.
  5. Brock JE. A note on the damped vibration absorber, *J Appl Mech (ASME)*, 1946; **13**: A-284.
  6. Den Hartog JP. *Mechanical Vibrations*, McGraw-Hill, 4th edition, New York, 1956.
  7. Crandall SH, Mark WD. *Random Vibration in Mechanical Systems*, Academic Press, New York, 1973.
  8. Warburton GB, Ayorinde EO. Optimum absorber parameters for simple systems, *Earthquake Eng Struct Dynam*, 1980; **8**: 197–217.
  9. Sadek F, Mohraz B, Taylor AW, Chung RM. A method of estimating the parameters of tuned mass dampers for seismic applications, *Earthquake Eng Struct Dynam*, 1997; **26**(6): 617–635.
  10. Park J, Reed D. Analysis of uniformly and linearly distributed mass dampers under harmonic and earthquake excitation, *Eng Struct*, 2001; **23**(7): 802–814.
  11. Wolf JP. *Soil–structure Interaction Analysis in Time Domain*, Prentice-Hall, New Jersey, 1988.
  12. Xu YL, Kwok KCS. Wind induced response of soil–structure–damper systems, *J Wind Eng Ind Aerod*, 1992; **43**(3): 2057–2068.
  13. Wu JN, Chen GD, Lou ML. Seismic effectiveness of tuned mass dampers considering soil–structure interaction, *Earthquake Eng Struct Dynam*, 1999; **28**(11): 1219–1233.
  14. Liu MY, Chiang WL, Hwang JH, Chu CR. Wind-induced vibration of high-rise building with tuned mass damper including soil–structure interaction, *J Wind Eng Ind Aerod*, 2008; **96**: 1092–1102.
  15. Thomson WT, Dahleh MD. *Theory of Vibration with Applications*, Prentice Hall Inc., 5th edition, London, 1997.
  16. Newmark NM. A method of computation for structural dynamics, *J Eng Mech (ASCE)*, 1959; **85**(EM3): 67–94.
  17. Dorigo M, Gambardella LM. Ant Colony System: A cooperative learning approach to the traveling salesman problem, *IEEE Trans Evol Comput*, 1997; **1**(1): 53–66.
  18. Kaveh A, Talatahari S. A particle swarm ant colony optimization for truss structures with discrete variables, *J Constr Steel Res*, 2009; **65**: 1558–1568
  19. Kaveh A, Talatahari S. Particle swarm optimizer, ant colony strategy and harmony search scheme hybridized for optimization of truss structures, *Comput Struct*, 2009; **87**: 267–283
  20. Abachizadeh M, Kolahan F. Evaluating the discretization of search space in continuous problems for ant colony optimization, *37th International Conference on Computers and Industrial Engineering (CIE 37th)*, Alexandria, Egypt, 2007.
  21. Karaboga D. An Idea Based on Honey Bee Swarm for Numerical Optimization, *Technical report*, Erciyes University, Turkey, 2005.
  22. Basturk B, Karaboga D. An Artificial Bee Colony (ABC) Algorithm for Numeric Function Optimization, *IEEE Symposium on Swarm Intelligence*, Indianapolis, IN,

- USA, 2006.
23. Basturk B, Karaboga D. On the Performance of Artificial Bee Colony (ABC) Algorithm, *Appl Soft Comput*, 2008; **8**: 687-697.
  24. Duan Q, Gupta VK, Sorooshian S. A shuffled complex evolution approach for effective and efficient optimization, *J Optim Theor Appl*, 1993; **76**(3): 501-521.
  25. Duan Q, Sorooshian S, Gupta VK. Optimal use of the SCE-UA global optimization method for calibrating watershed models, *J Hydrol*, 1994; **158**: 265-284.
  26. Sorooshian S, Duan Q, Gupta VK. Calibration of conceptual rainfall-runoff models using global optimization: application to the Sacramento soil moisture accounting model, *Water Resource Reservoirs*, 1993; **29**(4): 1185-1194.
  27. Nelder JA, Mead R. A Simplex method for function minimization, *Computer Journal*, 1965; **7**: 308-313.
  28. Guclu R, Yazici H. Vibration control of a structure with ATMD against earthquake using fuzzy logic controllers, *J Sound Vib*, 2008; **318**: 36-49.